Journal of NeuroVirology (2000) 6, 33–45

www.jneurovirol.com

A multi-mutant herpes simplex virus vector has minimal cytotoxic effects on the distribution of filamentous actin, α-actinin 2 and a glutamate receptor in differentiated PC12 cells

Kevin D Holmes[1,4], Aly K Cassam[2], Bosco Chan[3,4], Andrew A Peters[1,4], Lynne C Weaver[2] and Gregory A Dekaban*[,1,4]

[1]Gene Therapy and Molecular Virology Group, The John P. Robarts Research Institute, London, Ontario, N6A 5K8, Canada; [2]Neurodegeneration Research Group, The John P. Robarts Research Institute, London, Ontario, N6A 5K8, Canada; [3]Transplantation-Immunobiology Group, The John P. Robarts Research Institute, London, Ontario, N6A 5K8, Canada and [4]Department of Microbiology and Immunology, University of Western Ontario, London, Ontario, N6A 5K8, Canada

To develop effective gene therapy techniques that target populations of neurons in the spinal cord, suitable vectors must be developed that will undergo efficient, retrograde transport from an appropriate peripheral site and will not be cytotoxic. Our previous work (LeVatte *et al*, 1998a) has demonstrated that a replication defective herpes simplex virus vector 14HΔ3*vhsZ*, that has been substantially detoxified, is retrogradely transported from peripheral sites and can infect large numbers of the targeted spinal neurons. We plan to develop targeted gene therapy approaches designed to modulate the excitatory glutamatergic methyl-D-aspartate (NMDA) receptor in spinal cord neurons as a means of ameliorating a form of episodic high blood pressure that occurs after spinal cord injury. In this report, we demonstrate that, in differentiated PC12 cells, a neuronal-like cell line, the virus vector does not appear to alter aspects of the cytoskeletal architecture important to the proper distribution of the NMDA receptor. In turn, the distribution of endogenous NMDA receptor 1 subunit protein (NMDAR1) or a transfected NMDAR1-green fluorescent fusion protein was also found to be unaltered after vector infection. However, whereas endogenous NMDAR1 distribution was maintained, vector infection did tend to reduce the level of its expression. This drop in endogenous NMDAR1 expression coincided with the expression of the HSV immediate early genes ICP0 and ICP27 over the first 24–48 h. These results indicate that the 14HΔ3*vhsZ* herpes simplex virus vector is suitable to use in future strategies to alter the level of gene expression in targeted populations of spinal cord neurons. *Journal of NeuroVirology* (2000) **6,** 33–45.

Keywords: herpes simplex virus (HSV); vector; actin; α-actinin-2; N-methyl-D-aspartate receptor; PC12 cells

Introduction

Viral vectors have been used for a number of different applications within the central nervous system such as tract tracing (Mabon *et al*, 1997; LeVatte *et al*, 1997, 1998a,b; Clarke *et al*, 1998) and delivering genes encoding neurotrophic factors (Geschwind *et al*, 1994), enzymes (Geller *et al*, 1995) and glutamate receptors (Neve *et al*, 1997) to neurons. Our goal is to use viral vectors to alter glutamate receptor expression and anchoring in populations of spinal cord sympathetic preganglionic neurons (SPN) responsible for blood pressure control. In particular, we wish to diminish the pathological glutamatergic excitation of SPNs after spinal cord injury as a means of controlling autonomic dysreflexia, a hypertensive condition that can have serious life threatening consequences

*Correspondence: GA Dekaban
Received 19 November 1998; revised 11 August 1999; accepted 20 September 1999

(Krassioukov and Weaver, 1995, 1996; Krenz and Weaver, 1998; Llewellyn-Smith *et al*, 1997; Maiorov *et al*, 1997; Weaver *et al*, 1997; Sucher *et al*, 1993). Glutamate is the major excitatory neurotransmitter normally controlling SPNs and this appears to remain true after cord injury. Pharmacological blockade of the N-methyl-D-aspartate (NMDA) and α-amino-3-hydroxy-5-methyl-4-isoxazole proprionic acid (AMPA) spinal glutamate receptors substantially attenuated autonomic dysreflexia in a rat spinal cord injury model, each contributing nearly equally (Maiorov *et al*, 1997). In an effort to address the molecular mechanisms behind autonomic dysreflexia, we plan to alter glutamate receptor gene expression in specific populations of SPNs. In particular, we wish to alter N-methyl-D-aspartate (NMDA) receptor gene expression for two reasons. First, the NMDA receptor mediates a large portion of the glutamatergic excitation of SPNs after spinal cord injury (Maiorov *et al*, 1997). Second, the splice variants of the NMDA receptor subunits are more clearly defined in the spinal cord than those for the AMPA receptor (Furuyama *et al*, 1993; Luque *et al*, 1994; Tolle *et al*, 1993). To target such a specific population of SPNs requires peripheral inoculation of a suitable gene-transducing vector for retrograde neuronal transport because the SPNs are organized in a narrow column that extends the entire length of the thoracolumbar spinal cord. Aside from the physical barrier presented by the vertebral column, the multi-segmented distribution of SPNs throughout the spinal cord makes it impractical to access them by intraspinal injection. Axons of these SPNs converge in ganglia and peripheral organs that can be used as sites for vector inoculation.

Herpes simplex virus type 1 (HSV) vectors are particularly suitable for an application targeting a specific population of neurons as they are neurotropic and are retrogradely transported from the periphery. For gene delivery to spinal cord SPNs we have chosen to use an attenuated replication defective HSV, 14HΔ3*vhs*Z that contains three major mutations (Johnson and Friedman, 1994). The 14HΔ3*vhs*Z virus vector has both copies of the gene encoding infected cell protein 4 (ICP4) deleted and the transcriptional activation domain of virus protein 16 (VP16) has been destroyed, rendering the virus replication incompetent. These two genes, that regulate immediate early viral gene transcription, cause a large proportion of HSV-mediated toxicity (Johnson *et al*, 1994; Glorioso *et al*, 1995b; Russell *et al*, 1987). In addition, the *vhs* gene, encoding a virus-host shut-off protein that inhibits host cell protein synthesis, has also been inactivated by insertion of a β-galactosidase marker gene. Johnson *et al* (1994) observed that the cytotoxic effects of 14HΔ3*vhs*Z were markedly attenuated in fibroblast cells *in vitro*. Recently we reported that this vector appears to be minimally cytotoxic in a neuronal-like cell line, differentiated pheochromocytoma 12 (PC12) cells for up to 96 h post infection at MOI's of 1 and 10 (LeVatte *et al*, 1998a). We also demonstrated that, *in vivo*, the 14HΔ3*vhs*Z vector is not cytotoxic to SPNs after retrograde transport from the periphery. Furthermore, the inflammatory response to the vector-infected cells is greatly reduced compared to that observed previously for replication competent or tk^- mutant recombinant HSV vectors (LeVatte *et al*, 1997, 1998a). The small inflammatory response to 14HΔ3*vhs*Z vector infection in the spinal cord may be indirectly responsible for any remaining cytopathic effects since several pro-inflammatory cytokines can be toxic (Leib and Olivo, 1993; Martin *et al*, 1995; Oger and Dekaban, 1995; Wood *et al*, 1994). We have recently demonstrated that this remaining inflammatory response can be largely prevented through immunosuppression of the rats by cyclosporin A, a treatment that also accentuates vector-driven recombinant gene expression (Mabon *et al*, 1999).

A successful strategy to alter glutamate receptor expression must employ a vector that does not adversely affect the glutamate receptor and associated protein-protein interactions. For example, cytoskeletal proteins such as intact actin microfilaments and actin binding proteins such as alpha-actinin 2 are extremely important to the distribution and anchoring of glutamate receptors, such as the NMDA receptor, within the plasma membrane and at post synaptic terminals (Allison *et al*, 1998; Wyszynski *et al*, 1998; Sheng and Wyszynski, 1997). Although much is known about the detrimental effects of wildtype HSV viruses on cytoskeletal proteins (Becker *et al*, 1993; Norrild *et al*, 1986; Heeg *et al*, 1986), very little information exists about the effects of attenuated replication defective recombinant HSV vectors on glutamate receptors and their association with the cytoskeleton within an infected neuron. Clearly, HSV vectors that deliver functional or mutated glutamate receptor genes to neurons will only be successful if the cytotoxic effects of the HSV vector on the normal distribution of glutamate and other receptors and on the cytoskeleton are minimized.

The purpose of the present study was to compare HSV vector-associated cytotoxicity on the NMDA receptor 1 subunit (NMDAR1) distribution and on cellular proteins known to be involved in the appropriate distribution of NMDA receptors in neurons. In this study we will compare the 14HΔ3*vhs*Z vector to replication competent HSV vectors expressing all immediate early genes. Specifically we examined the effects of these viral vectors on the cellular localization of actin microfilaments, alpha-actinin 2, cell surface integrin expression and endogenous NMDAR1. In addition, we examined the effect of these viral vectors on the distribution and expression of a recombinant NMDAR1 tagged with enhanced green fluorescent protein (EGFP) transfected into differentiated PC12

cells. Our results indicated that 14HΔ3*vhs*Z may be an appropriate vector to deliver recombinant NMDA receptors to spinal cord neurons.

Results

Uniformity of virus infection by tk$^-$lacZ *HSV and 14HΔ3*vhs*Z*

We used a mutant HSV (tk$^-$*lacZ* HSV) with known cytotoxicity as a standard to which the cytotoxic effects of the 14HΔ3*vhs*Z could be compared. Our previous studies with this tk$^-$*lacZ* HSV have demonstrated its cytotoxicity *in vitro* and *in vivo* (LeVatte *et al*, 1997, 1998a). To be assured that the tk$^-$*lacZ* HSV and the 14HΔ3*vhs*Z infected cells with relatively equal efficiencies, 400, 800, and 2000 plaque forming units (pfu) of both viruses were plated on differentiated PC12 cells and RK13 cells and both resulted in the expected number of infected cells. Since the 1×10^9 pfu/ml stock of 14HΔ3*vhs*Z was titered on replication permissive E5 cells, we confirmed that similar titers would be obtained on the two replication non-permissive cells lines used in this study. These lines were rabbit kidney 13 (RK13) cells that had been used to titer the tk$^-$*lacZ* HSV and differentiated PC12 cells that were used for the rest of the experiments in this study. We obtained comparable titers of 7×10^8 pfu/ml and 4.3×10^8 pfu/ml on RK13 and differentiated PC12 cells respectively. Based on the titer on differentiated PC12 cells, 1.5 to 2.5×10^5 differentiated PC12 cells were infected at an MOI of 0.1, 1 and 10 resulting in infection of 7–10%, 65–80% and 95–100% of the cells, respectively (see Figure 1). This is similar to our previously reported observations for the infectivity of tk$^-$*lacZ* HSV and 14HΔ3*vhs*Z (LeVatte *et al*, 1998a,b).

Effect of virus infection on the distribution of actin microfilaments

In control, mock-infected differentiated PC12 cells, positive phalloidin staining was observed in the cell body surrounding the nucleus, in the neurites and also in growth cones (Figure 2A), indicating the presence of intact actin microfilaments in these compartments. Forty-eight (not shown) and 96 h (Figure 2B) after infecting differentiated PC12 cells with 14HΔ3*vhs*Z at a multiplicity of infection (MOI) of 10, the pattern of phalloidin staining had not changed compared to control cells.

Conversely, 48 h after infecting differentiated PC12 cells with *tk*$^-$*lacZ* HSV, at a MOI of 1 (data not shown) and 10 (Figure 2C), the cells were rounded with very short neurites, if any. Occasionally, in some cells, phalloidin fluorescence was observed in a thin perinuclear ring whereas the majority of cells were phalloidin negative, indicating the complete disaggregation of actin microfilaments in these cells.

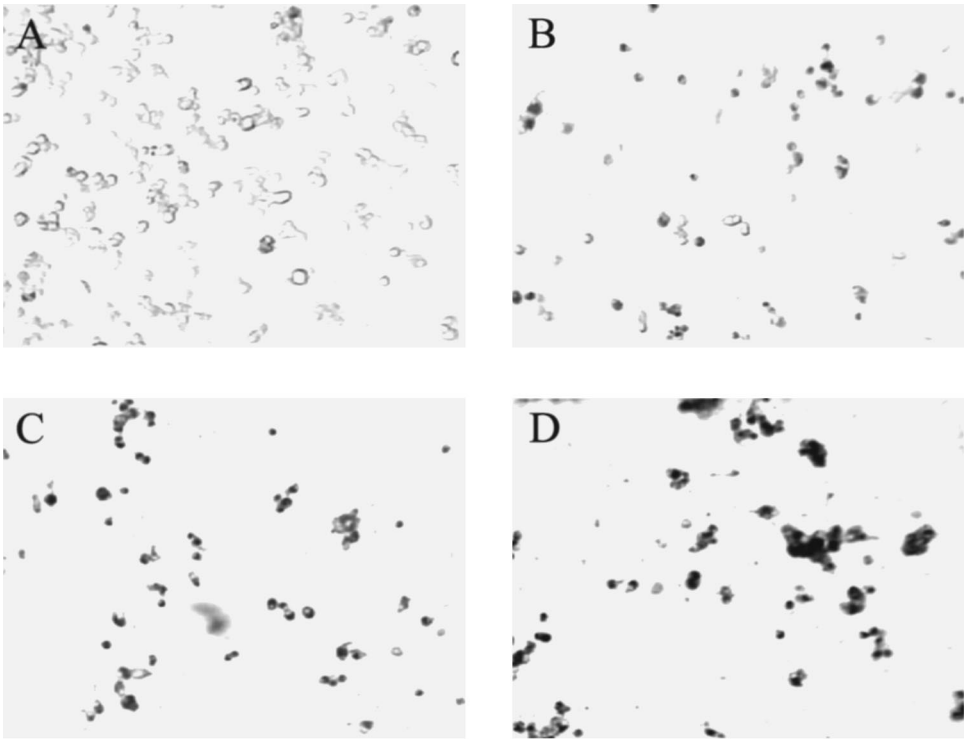

Figure 1 Expression of β-galactosidase activity 48 h after 14HΔ3*vhs*Z infection of differentiated PC12 cells at a MOI of 0 (**A**), 0.1 (**B**), 1 (**C**) and 10 (**D**) showing that 0, 7–10%, 65–80% and 95–100% of the cells, respectively, are infected.

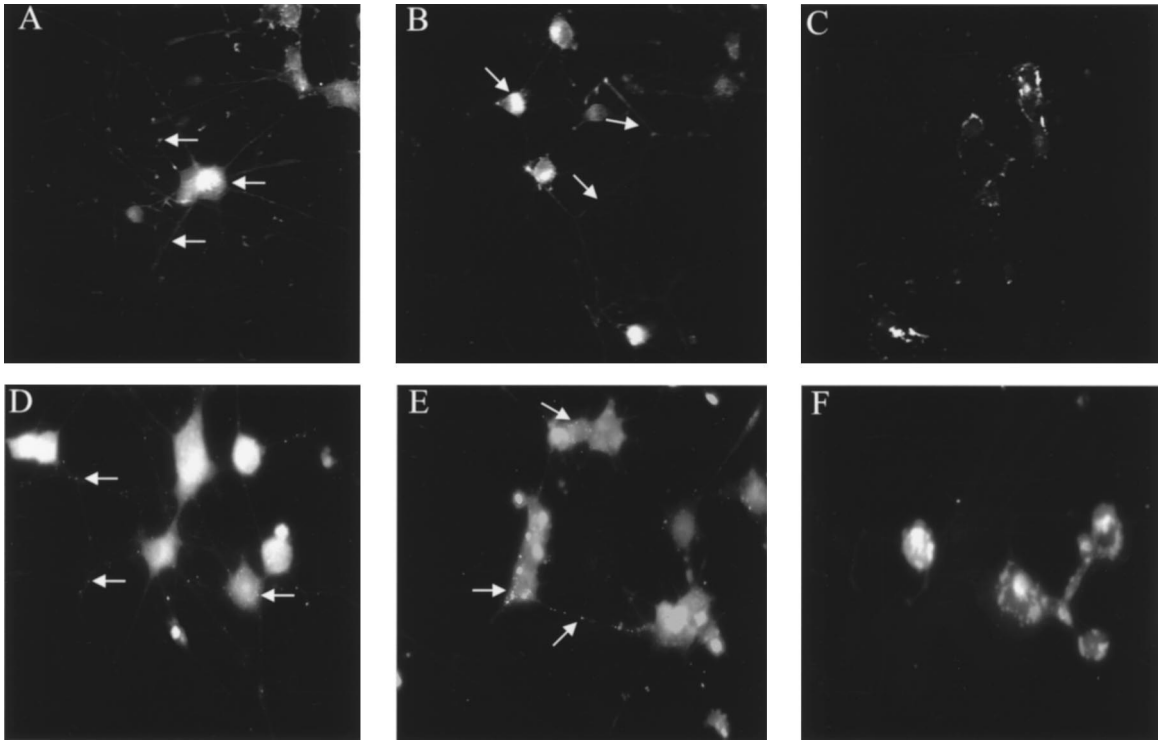

Figure 2 Distribution of phalloidin-TRITC (**A**–**C**) or alpha-actinin 2 immunoreactivity (**D**–**F**) in differentiated PC12 cells infected with either 14HΔ3*vhs*Z (**B**,**E**) or *tk*⁻*lacZ* HSV (**C**,**F**). Compared to mock-infected cells (**A**) the distribution of phalloidin-TRITC in the cell bodies and processes of differentiated PC12 cells (**A**,**B**, arrows) was unaltered following infection with 14HΔ3*vhs*Z for 96 h at an MOI of 10. Similarly, α-actinin 2 immunoreactivity was distributed as puncta throughout the cell bodies and processes of both mock- (**D**, arrows) and 14HΔ3*vhs*Z-infected (96 h, MOI 10) PC12 cells (**E**, arrows). The distribution of phalloidin-TRITC and α-actinin 2 in PC12 cells infected with *tk*⁻*lacZ* HSV at a MOI of 10 for 48 h are shown in (**C**) and (**F**) respectively. Phalloidin-TRITC appears to be restricted to clumps in the cell body within cells infected *tk*⁻*lacZ* HSV (**C**), and no fluorescence can be observed in the few remaining processes of these cells (**C**). Similarly, the punctate distribution of α-actinin 2 immunoreactivity is restricted to the cell body of cells infected with *tk*⁻*lacZ* HSV (**F**).

Effect of virus infection on the distribution of α-actinin 2

In uninfected, differentiated PC12 cells, puncta of α-actinin 2 immunoreactivity were observed in processes, growth cones and along the inner plasma membrane extending around the cell soma (Figure 2D). In differentiated PC12 cells 24, 48 and 96 h after infection with 14HΔ3*vhs*Z, at a MOI of 1 (not shown) and 10 (Figure 2E), the same pattern of immunofluorescence was observed. Conversely, α-actinin 2 was primarily observed only as puncta at the perimeter of the somata of differentiated PC12 cells infected with *tk*⁻*lacZ* HSV for 48 h (Figure 2F).

Effect of viral infection on the distribution of α1 and β1 integrins

The effects of *tk*⁻*lacZ* HSV and 14HΔ3*vhs*Z on expression of $\alpha1\beta1$ and overall $\beta1$ integrins on differentiated PC12 at 24, 48 and 96 h after infection was determined using flow cytometry. A representative experiment (n=3) is presented in Figure 3. The results reveal no significant change in either $\alpha1\beta1$ or overall $\beta1$ expression levels between cells that were mock infected and cells infected with the 14HΔ3*vhs*Z at an MOI of 10 at 24 (data not shown), 48 and 96 h. Similarly, in comparison with the mock-infected differentiated PC12 cells, no significant difference was seen in the level of either $\alpha1\beta1$ or overall $\beta1$ integrins expressed on the cell surface was observed at 24 (data not shown) or 48 h after infection with *tk*⁻*lacZ* HSV.

Distribution of endogenous NMDA receptors following vector infection

In controls mock-infected differentiated PC12 cells NMDAR1 immunoreactivity was observed in a pattern similar to the distribution of alpha-actinin 2. NMDAR1 immunofluorescence was distributed throughout the soma, but not the nucleus of differentiated PC12 cells. Punctate dots of immunofluorescence were also observed in long neurites extending from the somata (Figure 4A). No immunoreactivity was observed in the growth cones of these neurites. The pattern of endogenous NMDAR1 immunofluorescence did not change in differentiated PC12 cells 24 (not shown), 48 (not shown) and

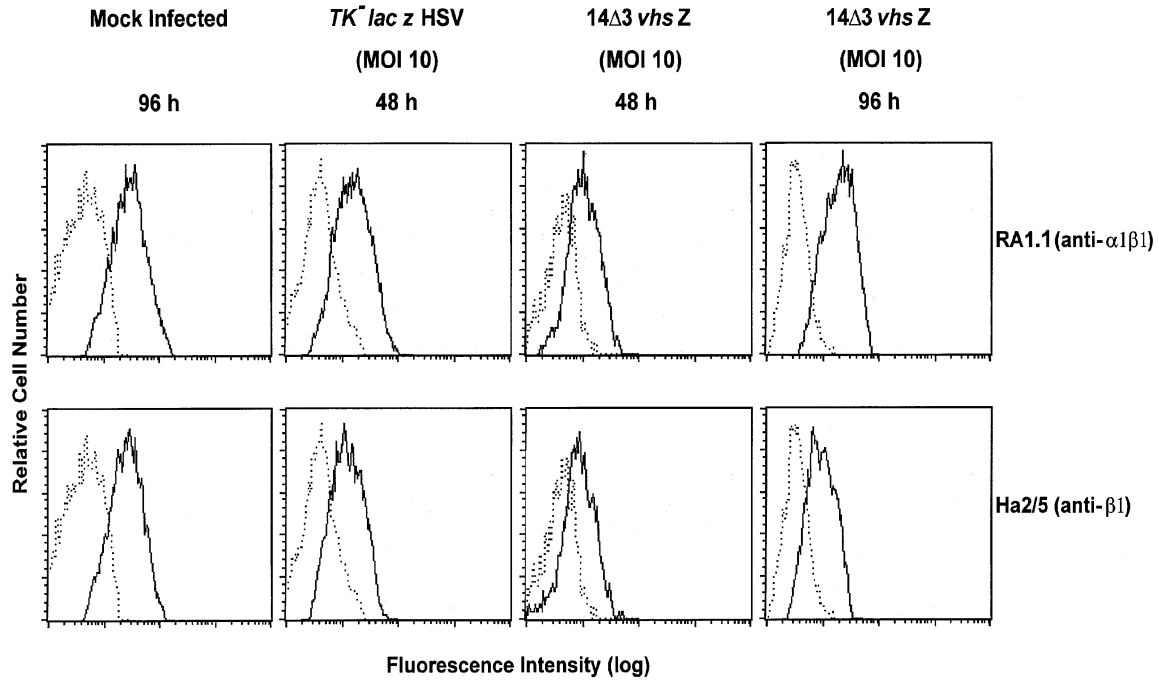

Figure 3 Effect of viral infection on $\alpha1\beta1$ and overall $\beta1$ integrin expression on differentiated PC12 cells. Compared to mock-infected cells, no significant increase in either $\alpha1\beta1$ or overall $\beta1$ integrin expression was observed at 48 and 96 h after infection with either *tk*$^{-}$*lacZ* HSV or 14HΔ3*vhs*Z at an MOI of 10. Dashed lines indicate immunostaining using an isotype matched control antibody, solid lines indicate specific immunostaining using mAb to rat $\alpha1\beta1$ or rat $\beta1$ integrin subunit.

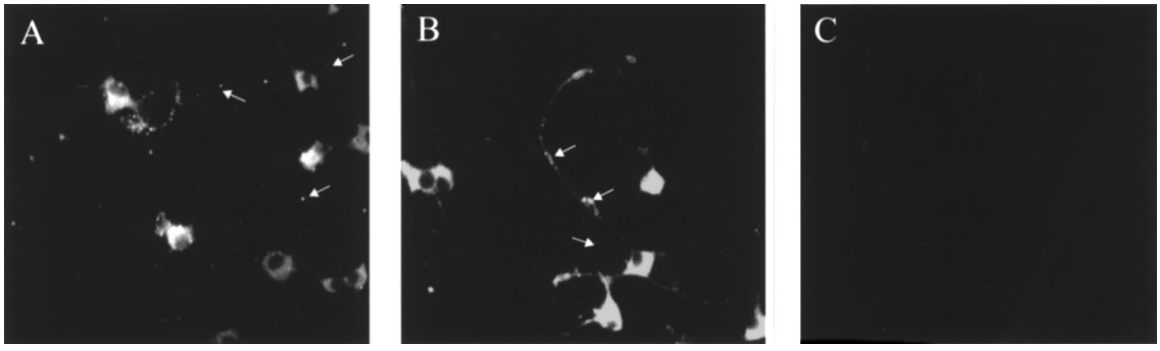

Figure 4 Distribution of endogenous NMDA receptor immunofluorescence in mock- (**A**) and vector-infected differentiated PC12 cells 96 h after infection with 14HΔ3*vhs*Z at a MOI of 10. In both groups of cells, punctate immunofluorescence was observed in neurites (**A**, **B**, arrows). A diffuse pattern of immunoreactivity was also observed in the soma of both groups of cells. (**C**) An example of cells that were not incubated with primary antibody against NMDAR1.

96 h (Figure 4B) after infection with 14HΔ3*vhs*Z at a MOI of 10. Conversely, very little immunofluorescence could be detected 48 h (not shown) after infection with *tk*$^{-}$*lacZ* HSV. Occasionally, puncta of immunofluorescence were observed around the cell body, but they were not observed in any of the retracted neurites associated with these cells. A control showing the specificity of the fluorescence in Figure 4A,B is presented in Figure 4C in which only the secondary antibody was used.

Effect of virus on the distribution of NMDAR1-EGFP in transfected differentiated PC12 cells

NMDAR1-EGFP was observed in discrete clusters throughout the cell body and neurites of mock-infected differentiated PC12 cells (Figure 5A) 48 h after transfection with a plasmid encoding a NMDAR1-EGFP fusion protein. The punctate distribution of NMDAR1-EGFP throughout much of the cytoplasm and in the neurites was unaltered 24, 48, and 96 h (Figure 5B) after infecting the transfected

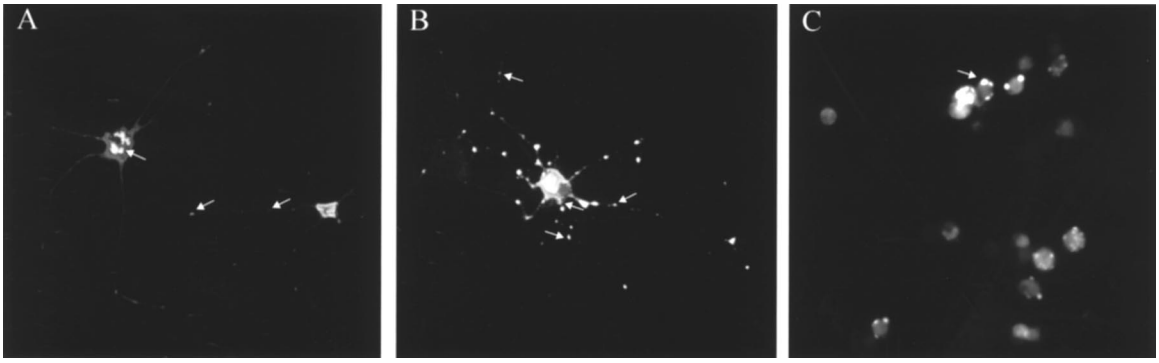

Figure 5 Distribution of NMDAR1-EGFP fusion protein, in mock- (**A**) and virus-infected differentiated PC12 cells 96 h after infection with 14HΔ3*vhs*Z at an MOI of 10 (**B**). Viral infection was performed 48 h after transfecting differentiated PC12 cells with pNMDAR1-EGFP. The neuronal morphology of differentiated PC12 cells was unaltered in mock-(**A**) or 14HΔ3*vhs*Z-infected cells (**B**). NMDAR1-EGFP was observed in puncta along the length of their processes (**A**, **B**, arrows). Conversely, NMDAR1-EGFP fluorescence was restricted to the puncta within the cytoplasm of cells infected with wild type virus for 48 h at an MOI of 10 (**C**, arrows).

cells with 14HΔ3*vhs*Z at a MOI of 10. Furthermore, the neuronal morphology of infected cells was unaffected by the presence of the HSV vector and the transfection reagent, lipofectamine. Conversely, cells infected with *tk*$^-$*lacZ* HSV (Figure 5C) had shortened processes and exhibited round morphology with the NMDAR1-EGFP fusion protein present in discrete round puncta (Figure 5C).

Effect of virus infection on endogenous NMDAR1 and NMDAR1-EGFP expression

A Western blot analysis of transiently transfected differentiated PC12 cells (Figure 6A) was carried out to determine whether vector infection negatively affected the levels of endogenous NMDAR1 and NMDAR1-EGFP expression. Densitometry was used to quantify the level of NMDAR1-EGFP expression after normalization for protein content and transfection efficiency by measuring luciferase activity from a co-transfected luciferase reporter plasmid (Figure 6B). Virus infection was carried out 48 h after the transfection was completed and thus the time points shown in Figure 6 were, in fact, collected 72, 96 and 114 h post-transfection. The level of NMDAR1-EGFP expression was unchanged at 24 and 48 h, ($P > 0.1$) whether the cells were infected or not. By 96 h postinfection, NMDAR1-EGFP expression had declined ($P < 0.01$). Virus vector infection increased the absolute amount of NMDAR1-EGFP by twofold ($P < 0.01$) over that observed in non-infected cells at 24 and 48 h post infection when transfection efficiency was taken into account.

The expression of endogenous NMDAR1 in mock-infected cells was not significantly ($P > 0.1$) altered during the 24 – 96 h period although expression tended to become reduced by 96 h. Endogenous NMDAR1 expression in virus vector-infected cells (Figure 6) also did not change with time. Virus vector-infected cells, when compared to non-infected cells at the same time points, showed reduced endogenous NMDAR1 expression at 24 and 48 h after infection ($P < 0.05$). Depending on the experiment, this reduction varied from 2 – 5-fold.

It is likely that the drop in the levels of endogenous NMDAR1 gene protein expression at 2 and 48 h post infection was due to the actions of the remaining immediate early genes present in 14HΔ3*vhs*Z on the host cell. The levels of expression of the remaining immediate early genes have not been previously reported for 14HΔ3*vhs*Z. Therefore we examined the expression of two of the remaining immediate early genes, ICP0 and ICP27, in Vero, RK13, and differentiated PC12 cells infected with either 14HΔ3*vhs*Z or tk-*lacZ* HSV at an MOI of 1 and 10. As shown in Figure 7, maximal levels of the immediate early proteins ICP0 and ICP27 occurred at 24 h and then decreased at 48 and 96 h post-infection in both RK13 cells and in differentiated PC12 cells. After infection by 14HΔ3*vhs*Z, ICP0 and ICP27 were expressed to greater extents in the differentiated PC12 cells than in the RK 13 cells. Vero cells, which are known to be more permissive for HSV gene expression and replication, appeared to sustain 14HΔ3*vhs*Z ICP0 and ICP27 expression at higher levels, similar to that observed in RK13 cells after infection by *tk*$^-$*lacZ* HSV (Figure 7B,C).

Discussion

We have demonstrated that a replication defective, substantially detoxified herpes simples virus vector, 14HΔ3*vhs*Z, has a minimal impact on aspects of cytoskeletal architecture important to the normal distribution of glutamate receptors such as the NMDA receptor in neuronal-like cells. Filamentous actin and α-actinin 2 both retained a normal distribution in vector-infected cells and, in turn, the normal distribution of the NMDAR1 was also

maintained. Furthermore, the cell surface expression levels of the major integrins ($\alpha 1\beta 2$) involved in differentiated PC12 cell adhesion (Arregui *et al*, 1994; Tomaselli *et al*, 1990) to the subcellular

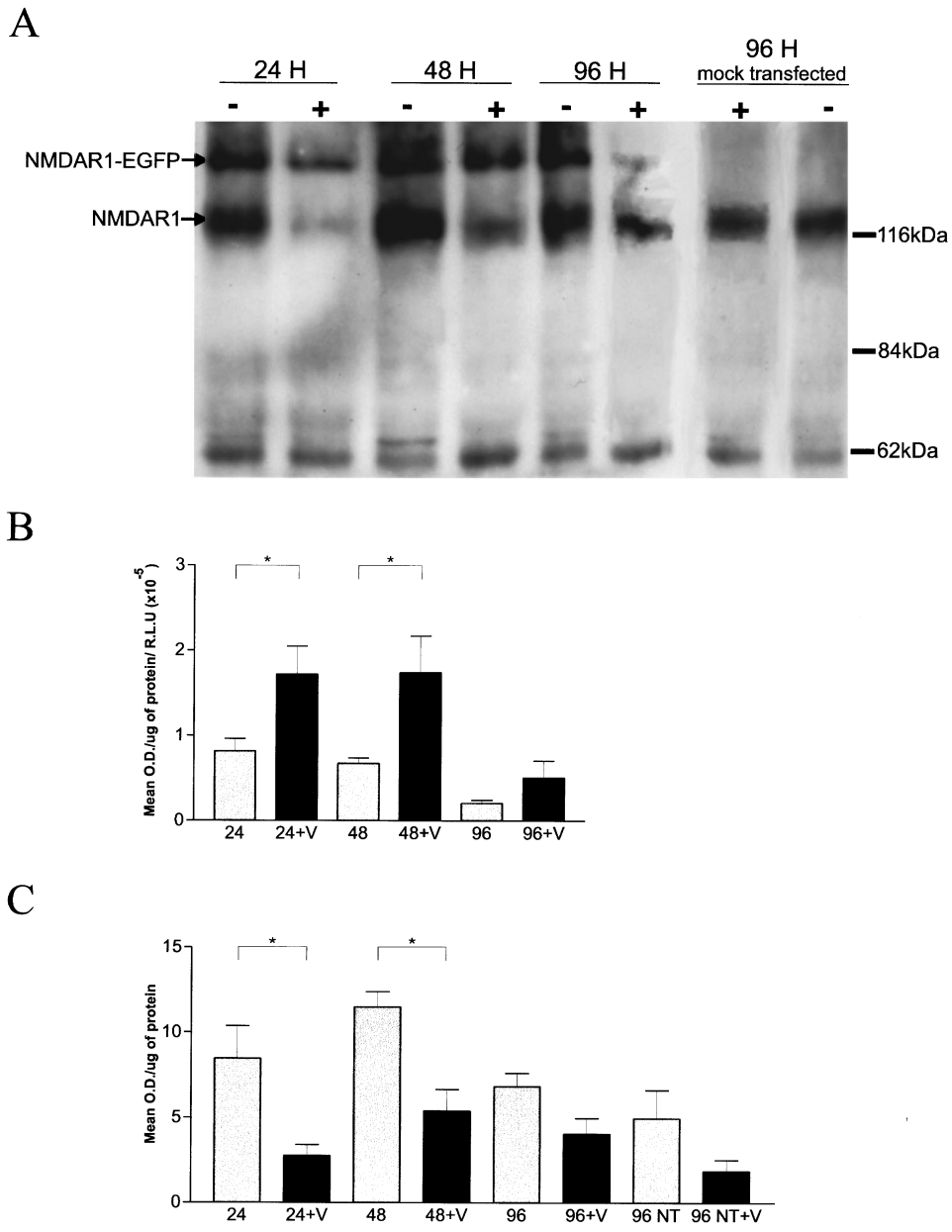

Figure 6 Effect of 14H3*vhs*Z vector infection on the expression of transfected NMDAR1-EGFP and endogenous NMDAR1. (**A**) Western blot analysis demonstrating levels of transfected NMDAR1-EGFP or endogenous NMDAR1 protein in differentiated PC12 cells after mock infection (indicated by − above respective lane) or after infection by 14HΔ3*vhs*Z at a MOI of 10 (indicated by + above respective lane) 24, 48 or 96 h after infection. Mock and virus vector infection of all cells occurred 48 h after the transfection was completed. (**B**) Densitometric analysis of NMDAR1-EGFP expression in the presence (+V) or absence of 14HΔ3*vhs*Z vector 24, 48, and 96 h after infection. Data represent mean optical densities (O.D.)/μg of protein/relative luciferase unit (R.L.U) $\pm$ standard error of the mean (s.e.m.). The level of NMDAR1-EGFP expression in mock-infected cells was not significantly different at 24, 48, 96 h post infection ($P > 0.1$). In virus vector-infected cells the NMDAR1-EGFP expression was not significantly different between 24 and 48 h post-infection ($P > 0.1$), but at 96 h post infection NMDAR1-EGFP expression was significantly reduced when compared to the expression observed at either 24 or 48 h post-infection ($P > 0.01$). Asterisks indicate that the level of NMDAR1-EGFP expression between virus vector-infected and mock-infected cells was significantly different at a given time point ($P < 0.01$). (**C**) Densitometric analysis of endogenous NMDAR1 expression in the presence (+V) or absence of 14HΔ3*vhs*Z vector 24, 48, and 96 h after infection. NT represents non-transfected controls. Data represent mean O.D. $\pm$ s.e.m./μg of protein. Endogenous NMDAR1 expression in mock-infected cells was not significantly different at 24, 48 and 96 h post-infection ($P > 0.1$). The same was true for virus vector-infected cells ($P > 0.1$). Asterisks indicate that the level of endogenous NMDAR1 expression between virus vector-infected and mock-infected cells was significantly different at a given time point ($P < 0.05$).

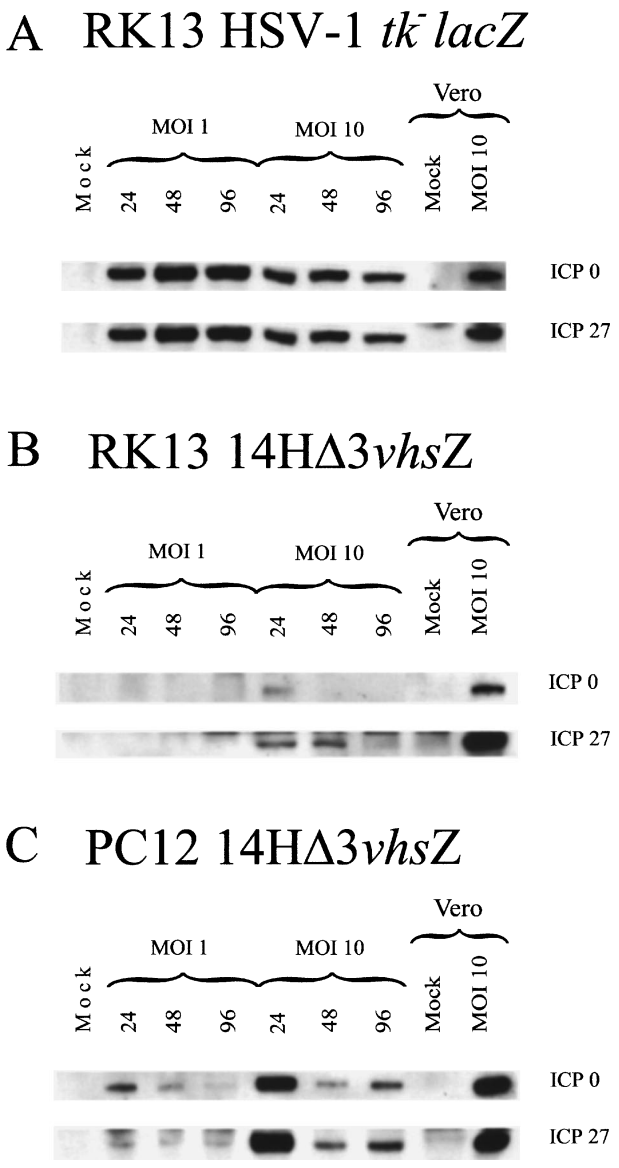

Figure 7 Expression of the HSV immediate early proteins ICP0 and ICP27 in infected RK-13, differentiated PC12 cells at a MOI of 1 and 10 over a 96 h time period post-infection. The time point shown for *tk⁻lac*Z HSV (**A**) and 14HΔ3*vhs*Z (**B** and **C**) infection of Vero cells for both the mock infection and the infection at a MOI of 10 is at 48 h post infection.

matrix were also unafffected. Thus, in preparation for developing 14HΔ3*vhs*Z as a gene transfer vector for spinal cord neurons *in vivo*, these results, in combination with our previously reported results (LeVatte *et al*, 1998a), demonstrate that this vector should be suitable for use in experimental systems. In preliminary studies we have already made recombinant 14HΔ3*vhs*Z carrying an anti-inflammatory gene from the myxoma poxvirus in two different locations (tk and gJ) in the viral genome. These quadruple mutants were easily obtained and grew to titers comparable to the parental 14HΔ3*vhs*Z (M LeVatte, GA Dekaban, LC Weaver and G McFadden, unpublished data). Thus, we anticipate that new 14HΔ3*vhs*Z vectors can be readily constructed.

Spinal cord injury disrupts regulatory input from the brain to neurons caudal to the site of injury. As a result the neurons caudal to the injury often become dysregulated, which in turn manifests itself in the form of pain syndromes (allodynia), spasticity and autonomic disturbances such as autonomic dysreflexia. A targeted gene therapy approach to populations of dysregulated neurons offers the potential to ameliorate some of the pathological consequences of spinal cord injury and may lead to an improved quality of life for the patient. By taking advantage of the HSV neurotropism and natural ability to undergo retrograde transport from peripheral sites to populations of neurons in ganglia or the spinal cord the potential for HSV-delivered gene therapy approach becomes testable. In addition, HSV establishes a natural latency in neurons from which it can normally be reactivated, whereas replication defective in HSV vectors suitable for gene therapy applications are forced into latency and cannot reactivate. While the exact process by which HSV establishes latency remains to be elucidated, once latency is established the virus genome is maintained as a nuclear episome and is physiologically and to a large extent immunologically silent (Fink *et al*, 1996; Glorioso *et al*, 1995a; Steiner and Kennedy, 1993). Our recent research has demonstrated that recombinant HSV vectors can indeed target sufficient numbers of neurons necessary to potentially elicit a physiologically detectable response *in vivo* (LeVatte *et al*, 1997, 1998a). While these vectors may not be clinically applicable for safety reasons, they do permit the testing of gene therapy concepts in appropriate animal models.

The 14HΔ3*vhs*Z HSV vector appears to be very suitable for the purpose of investigating gene therapy approaches for the treatment of spinal cord injury. This vector exhibits minimal levels of neuronal toxicity *in vitro* and *in vivo* (LeVatte *et al*, 1998a). In this current work, we examined the effects of 14HΔ3*vhs*Z vector infection on specific aspects of the neuronal cytoskeleton that have critical protein-protein interactions with the C-terminal domains of the NMDAR1 subunit, a future potential gene therapy target. Furthermore, many other receptors involved in neural synaptic transmission require an intact cytoskeleton for their proper distribution and function. Wildtype HSV is well known for its capacity to disrupt the cytoskeleton in infected cells (Cudmore *et al*, 1997; Elliot and O'Hare, 1998; Krempien *et al*, 1984; Norrild *et al*, 1986). Utilizing HSV vectors to disrupt the distribution/function of a single type of receptor, such as the NMDA receptors, will only be feasible if the vector does not affect the distribution of other receptors in the target neurons. Specifically, a vector must not adversely change the integrity of cytoskeletal proteins such as filamentous

actin (Sheng and Wyszynski, 1997) and α-actinin 2 (Wyszynski *et al*, 1998; Allison *et al*, 1998). Recently a number of studies have demonstrated the importance of these proteins and spectrin in the appropriate localization of a wide variety of receptors, such as NMDA and AMPA type glutamate receptors, to the post synaptic densities of the plasma membrane (Allison *et al*, 1998; Wyszynski *et al*, 1997, 1998; Krukoff *et al*, 1995; Wechsler and Teichberg, 1998). The distribution of many of these cytoskeletal proteins is completely altered in cells after infection with wildtype viruses (Krempien *et al*, 1984; Becker *et al*, 1993; Heeg *et al*, 1986; Johnson *et al*, 1992).

The results of our studies using differentiated PC12 cells suggested that infection with the replication defective 14HΔ3*vhs*Z HSV vector at a high MOI (10) did not adversely affect the distribution of actin microfilaments. Phalloidin was used to determine the effects of viral infection on the distribution of actin fibres within differentiated PC12 cells because phalloidin has been shown to bind only to intact or filamentous actin in a wide variety of cell types, including differentiated PC12 cells (Cornet *et al*, 1994; Sanders and Wang, 1991). However, these observations did not eliminate the possibility that vector infection caused subtle changes in the organization of filamentous actin that could alter the clustering or distribution of other actin binding proteins such as α-actinin 2 and neurotransmitter receptors, such as the NMDA receptor, on the plasma membrane.

Our experiments with 14HΔ3*vhs*Z infection did not demonstrate any changes in the distribution of α-actinin 2 in differentiated PC12 cells. Both filamentous actin and α-actinin 2 are known to interact with the C-terminal domains of NMDAR1 splice variants found in the spinal cord (Furukawa *et al*, 1997; Wyszynski *et al*, 1997, 1998). Our results also demonstrated that the distribution of endogenous NMDAR1 in 14HΔ3*vhs*Z-infected differentiated PC12 cells was not altered, although the Western blot analysis suggests that vector infection did result in a drop in the amount of endogenous NMDAR1 protein present as soon as 24 h after infection. These results are in marked contrast to the cytotoxic effects of the recombinant, replication competent HSV vectors (LeVatte *et al*, 1997, 1998a). In these studies actin filaments no longer bound phalloidin in most infected cells, indicating that the actin filaments had undergone depolymerization. Similarly, the normal distribution of α-actinin 2 and endogenous NMDAR1 was no longer apparent. Thus it would appear that, in 14HΔ3*vhs*Z-infected cells, the cytoskeletal architecture for proper NMDA receptor distribution is maintained. In addition, our results showed that no significant changes in the levels of $\alpha 1\beta 1$, the principle integrin on PC12 cells, after virus vector infection over a 96 h time period.

The current experiments did not permit us to determine whether the drop in NMDAR1 protein levels after vector infection occurs only in differentiated PC12 cells or if this drop will be a problem for neurons *in vivo*. This decrease in NMDAR1 expression coincides with residual expression of the remaining HSV immediate early genes (infected cell proteins ICP0 and ICP27) which are known to be cytotoxic (Johnson *et al*, 1992, 1994; Krisky *et al*, 1998). In some experiments we did not observe a partial recovery in NMDAR1 expression. A possible explanation for the unchanged distribution of NMDAR1 after virus vector infection despite a decrease in the absolute amount of NMDAR1 protein might be found in the recent results of Huh and Wenthold (Tanabe *et al*, 1995). These investigations described two pools of NMDAR1 in neurons, one rapidly turning over with a half-life of 2 h and a second with a very long half-life of 34 h. This latter pool associated with the plasma membrane and was part of the synaptic densities containing cytoskeletal protein complexes. The effects of 14HΔ3*vhs*Z on NMDAR1 protein levels were possibly greatest on the short-lived pool of NMDAR1 during the period in which this virus attempts to shut down host cell RNA and protein synthesis. Accordingly, the distribution of the longer-lived pool of NMDAR1 on the plasma membrane of the cell soma and neurites would not be affected.

Experiments were also performed to determine the effects of the 14HΔ3*vhs*Z on recombinant NMDAR1-EGFP fusion protein distribution and expression. The NMDAR1-EGFP distribution in transiently transfected differentiated PC12 cells was not altered upon infection with 14HΔ3*vhs*Z and was very similar to that of the endogenous NMDAR1 distribution. The Western blot analysis revealed that in the presence of the 14H3*vhs*Z infection, expression of the NMDAR1-EGFP was increased twofold, although endogenous NMDAR1 expression tended to decrease. This is likely due to the expression of the HSV immediate early gene ICP0, a transcriptional transactivator of viral promoters including the heterologous CMV immediate early promoter used to drive NMDAR1-EGFP expression. HSV vectors that lack ICP0 do not efficiently express recombinant genes from the CMV promoter (Shering *et al*, 1997; Krisky *et al*, 1998).

In summary, our observations clearly demonstrate that a multi-mutant HSV vector, 14HΔ3*vhs*Z, has limited cytotoxic effects on the distribution of certain cytoskeletal proteins and endogenous or transiently transfected NMDA receptors within neuronal-like differentiated PC12 cells. The expression of other cellular proteins, in addition to NMDAR1, appear to be reduced shortly after infection *in vitro* as a consequence of HSV infection (Rubenstein and Price, 1983, 1984;

Rubenstein *et al*, 1985). It remains to be determined, if after several days, NMDAR1 protein levels will return to normal. We do know that infection with 14HΔ3*vhs*Z did not result in the loss of any neurons *in vivo* (LeVatte *et al*, 1998a). These results indicate that this vector would be suitable for the delivery of recombinant receptor proteins to neurons *in vivo*. Future studies will be required to clarify the role of the remaining immediate early proteins in neuronal cytotoxicity *in vivo* to assure that the anticipated gene therapy effects are due to the transduced recombinant gene and not due to non-specific effects of the vector.

Materials and methods

Culturing cell lines
Routine culturing of undifferentiated PC12 cells and the differentiation of PC12 cells with NGF has been described previously (LeVatte *et al*, 1998a). Differentiation of the PC12 cells was allowed to proceed for at least 5 days before using them in an experiment. RK13 and Vero cells were maintained as previously described (LeVatte *et al*, 1997).

Preparation of virus stocks
14HΔ3*vhs*Z was originally obtained from Dr P Johnson (Johnson *et al*, 1994). The preparation and growth of 14HΔ3*vhs*Z (LeVatte *et al*, 1998a) and the two replication competent recombinant vectors have been described in detail previously (LeVatte *et al*, 1995, 1997). The titre of 14HΔ3*vhs*Z used in this study was 1×10^9 pfu/ml as determined on replication permissive E5 cells. The two replication competent recombinant vectors expressed β-galactosidase from either the Us5 gene (Us5gal/gJ *lac*Z) (LeVatte *et al*, 1995) or from the tk gene locus (*tk*$^-$*lacZ* HSV) (LeVatte *et al*, 1997). The titre of the gJ *lac*Z vector was 4.4×10^9 pfu/ml and of the tk$^-$*lac*Z HSV was 1×10^8 pfu/ml.

Virus infection
At least 5 days after being seeded into 6-well plates, a representative well from each plate was trypsinized with Tryspin-EDTA (Gibco-BRL, Grand Island, NY). The number of cells/well was counted using a Coulter Z cell counter (Coulter Electronics, LTd., Luton, England) to determine the amount of virus necessary to achieve the desired MOI and this number ranged between 1.5 to 2.5×10^5 cells per well. Differentiated PC12 cells were infected as described previously (LeVatte *et al*, 1998a) with 14HΔ3*vhs*Z at a MOI of 0 (mock-infected), 1 or 10 pfu/cell for 24, 48 or 96 h or with either *tk*$^-$*lac*Z HSV or gJ*lac*Z at MOIs of 0, 1 or 10 for 24 or 48 h.

Immunocytochemistry for endogenous NMDAR1, α-actinin 2 and actin filaments
After 24, 48 or 96 h of virus infection the medium was removed from both virus and mock-infected cells, and the cells were fixed with ice cold 95% ethanol/acetic acid (3 : 1) for 10 min. After 10 min the fixative was removed and the cells were washed twice with Tris-phosphate buffered saline (TPBS). Next the cells were incubated in a blocking solution containing TPBS and 10% normal horse serum for 45–60 min at room temperature. Subsequently, the blocking solution was removed and the cells were incubated in TPBS containing 5% normal horse serum and 1 : 1000 dilution of an anti-NMDAR1 murine monoclonal antibody (PharMingen Canada Inc., Missisauga, ON) diluted. This antibody recognizes a region between the third and fourth transmembrane regions of the NMDAR1 subunit that is common to all isoforms of the receptor. The cells were incubated in primary antibody for 48 h at room temperature. After 48 h the primary antibody was removed and the cells were washed twice in TPBS. The cells were then incubated in TPBS with 5% normal horse serum and a 1 : 200 dilution of biotinylated secondary antibody raised in donkey against mouse IgG1 (Jackson ImmunoResearch, West Grove, PA) for 16 h at room temperature. The secondary antibody was removed, and after two washes in TPBS, the cells were incubated in a TPBS solution containing 5% normal horse serum and a 1 : 200 dilution of lissamine rhodamine streptavidin (Jackson ImmunoResearch, West Grove, PA) for 3–4 h at room temperature. After removing the fluorochrome, the cells were washed twice and subsequently stored in TPBS.

Immunocytochemistry for α-actinin 2 was carried out in a similar fashion with the following modifications. The cells were fixed with 4% formaldehyde in TPBS for 10 min, washed twice with TPBS containing 0.3% Triton-X-100 (TPBS-X) and then blocked with TPBS-X containing 10% normal horse serum. A mouse monoclonal antibody against α-actinin 2 (1 : 500, Sigma, St. Louis, MO) was incubated with the cells for 72 h. The cells were washed and then incubated in biotinylated secondary antibody and lissamine rhodamine streptavidin as described above.

For the detection of intact actin filaments 24, 48 or 96 h post infection, the media was removed from both virus and mock-infected cells, and the cells were fixed with 4.0% formaldehyde in 0.1 M phosphate buffered saline (PBS) for 10 min at room temperature. After being washed twice with PBS, the cells were then permeabilized in a solution of TPBS containing 0.3% Triton-X-100 for 10 min at room temperature. After washing the cells in TPBS with 1% normal horse serum for 20 min, the cells were incubated in solution of phalloidin conjugated to rhodamine (Sigma, USA; diluted 1 : 5000), in TPBS with 1% normal horse serum for 35 min at room temperature. The TPBS/phalloidin solution was removed and the cells were washed twice with TPBS.

Fluorescence for the NMDAR1 subunit, α-actinin 2 and actin filaments was assessed using an Olympus IX70 inverted fluorescence microscope.

Flow cytometry
The expression of rat $\alpha1\beta1$ integrin on the surface of mock- and virus-infected differentiated PC12 cells was determined using the mouse monoclonal antibody (mAb) RA1.1 (Chemicon International, Temecula, CA). Similarly, the expression of the rat $\beta1$ integrin subunit was determined using the mAb HA2/5 (Pharmingen, San Diego CA). Cells harvested from culture plates by incubating with versine (0.5 mM EDTA, 137 mM NaCl, 2.68 mM KCl, 8 mM anhydrous Na_2HPO_4, 1.5 mM KH_2PO_4, 1.1 mM glucose, pH 7.4) were washed in PBS containing 1% bovine serum albumin and 0.01% sodium azide. The cells were then incubated with the specific mAb or isotype matched control mAb for 40 min at 4°C at 5 μg/ml, the predetermined saturating concentration. Next, the cells were washed and incubated with the corresponding FITC conjugated $F(Ab')_2$ fragments of the secondary antibodies. Results were analyzed using a Becton Dickinson FACScan as described (Ho *et al*, 1997).

Construction of pNMDAR1-EGFP and transfection of PC12 cells
The plasmid NF2(pNF2) was a gift of Dr TE Hughes (Marshall *et al*, 1995). We subsequently modified pNF2 to express the genetically engineered enhanced GFP (EGFP) in place of wildtype GFP. This was carried out by synthesizing two short oligonucleotides that were annealed to create a fragment beginning with a 5′ *Nhe*I restriction enzyme site and ending with a 3′ *PinA*I site. The synthetic fragment was cloned into *Nhe*I and *PinA*I digested pEGFP-N1 (Clontech, Palo Alto, CA) in order to place the EGFP sequence in frame with the NMDAR1 reading frame. The resulting plasmid was then cut with *Nhe*I and *Xba*I to excise the EGFP fragment and clone it into a similarly digested pNF2. The resulting pNMDAR1-EGFP was subjected to dideoxy sequencing on an ABI Model 377 automated DNA sequencer (ABI, Columbia, MD) to confirm that NMDAR1 was in frame with EGFP.

Following 5–6 days of differentiation with NGF, PC12 cells were co-transfected with an NMDAR1-EGFP fusion construct, pNMDAR1-EGFP, and a luciferase reporter plasmid (pCIG-2 luc, provided by Dr C Strathedee, Robarts Research Institute, London, Ontario) to monitor for transfection efficiency. Plasmid DNA (2 μg/well) and Lipofectamine (10 μl/well; Gibco-BRL, Grand Island, NY) were used to transfect differentiated PC12 cells essentially as described in the manufacturer's instructions. After transfecting the cells for 5 h, 1 ml of DMEM without NGF was added to each well. After a further 24 h at 37°C, the media was removed from each well and fresh media containing NGF was added. At 24, 48, and 96 h post infection, cells were examined under a Zeiss Axiovert 25 inverted fluorescence microscope with a mercury arc lamp (100 W) and a FITC filter set (consisting of a 480/40 nm excitation filter and a 535/50 emission filter) for detection of EGFP in live cells.

Electrophoresis and immunoblotting
At 24, 48 and 96 h post infection, differentiated PC12 cells were harvested and lysed in cell culture lysis reagent (Promega, Madison, WI). Protein concentrations for each sample were then determined in triplicate using the Bradford assay (BioRad, Mississauga, Ontario). Proteins were separated on either an 8% (for ICP0 and NMDAR1) or 15% (for ICP27) sodium dodecyl sulphate-poly acrylamide gel electrophoresis (SDS–PAGE) as previously described (Arp *et al*, 1993). Immunoblotting was performed using the Enhanced Chemiluminescence (ECL) method according to the manufacturer's instructions (Amersham, Oakville, Ontario). The mouse monoclonal anti-NMDAR1 antibody (Pharmingen, Mississauga, Ontario) recognizes an epitope between amino acids 660 and 811 of the NMDAR1 protein and was used at a dilution of 1 : 500. Mouse monoclonal antibodies for HSV ICP0 and ICP27 were obtained from the Goodwin Institute for Cancer Research (Plantation, Florida) and were both used at dilutions of 1 : 1000. The goat anti-mouse horseradish peroxidase (HRP)-conjugated secondary antibody (Sigma Chemical Co., St. Louis, MO) was used at a dilution of 1 : 7500. Exposed X-ray films were scanned in transmittance mode on Model GS700 imaging densitometer (BioRad, Mississauga, Ontario). The relative optical density for the endogenous NMDAR1 and NMDAR1-EGFP were normalized for transfection efficiency using a luciferase assay kit (Promega, Madison, WI) and protein content. A statistical analysis using two-way ANOVA was employed to determine if significant changes in expression had occurred with significance defined at $P \leqslant 0.05$.

Acknowledgements

This research was supported by grant NA-3342 from the Heart and Stroke Foundation of Ontario and AK Cassam was supported by a grant from the Medical Research Council of Canada. LC Weaver is a career investigator of the Heart and Stroke Foundation of Ontario. GA Dekaban was supported by an Ontario Ministry of Health Career Scientist Award. The views expressed in this paper are those of the authors and do not reflect those of the Ontario Ministry of Health.

References

Allison DW, Gelfand VI, Spector I, Craig AM (1998). Role of actin in anchoring postsynaptic receptors in cultured hippocampal neurons: differential attachment of NMDA versus AMPA receptors. *J Neurosci* **18:** 2423–2436.

Arp J, Ford CM, Palker TJ, King EE, Dekaban GA (1993). *J Gen Virol* **74:** 211–222.

Arregui CO, Carbonetto S, McKerracher L (1994). Characterization of neural cell adhesion sites: Point contacts are the sites of interaction between integrins and the cytoskeleton in PC 12 cells. *J Neurosci* **14:** 6967–6977.

Becker Y, Tavor E, Asher Y, Berkowitz C, Moyal M (1993). Effects of herpes simplex virus type-1 U_L41 gene on the stability of mRNA from the cellular genes: β-actin, fibronectin, glucose transporter-1, and docking protein, and on virus intraperitoneal pathogenicity to newborn mice. *Virus Genes* **7:** 133–143.

Clarke HA, Dekaban GA, Weaver LC (1998). Identification of lamina V and VII interneurons presynaptic to adrenal sympathetic preganglionic neurons in rats using a recombinant herpes simplex virus type 1. *Neurosci* **85:** 863–872.

Cornet M, Isobe Y, Lemanski LF (1994). Effects of anisosmotic conditions on the cytoskeletal architecture of cultured PC12 cells. *J Morphol* **222:** 269–286.

Cudmore S, Reckmann I, Way MJ (1997). Viral manipulations of the actin cytoskeletion. *Trends Microbiol* **5:** 142–148.

Elliot G, O'Hare P (1998). Herpes simplex virus type 1 tegument protein VP22 induces the stabilization and hyperacetylation of microtubules. *J Virol* **72:** 6448–6455.

Fink DJ, DeLuca NA, Goins WF, Glorioso JC (1996). Gene transfer to neurons using herpes simplex virus-based vectors. *Ann Rev Neurosci* **19:** 265–287.

Furukawa K, Fu W, Li Y, Witke W, Kwiatkowski DJ, Mattson MP (1997). The actin-severing protein gelsolin modulates calcium channel and NMDA receptor activities and vulnerability to excitotoxicity in hippocampal neurons. *J Neurosci* **17:** 8178–8186.

Furuyama T, Kiyama H, Sato K, Park HT, Maeno H, Takagi H, Tohyama M (1993). Region-specific expression of subunits of ionotropic glutamate receptors (AMPA-type, KA-type and NMDA receptors) in the rat spinal cord with special reference to nociception. *Mol Brain Res* **18:** 141–151.

Geller AI, During MJ, Oh YJ, Freese A, O'Malley K (1995). An HSV-1 vector expressing tyrosine hydroxylase causes production and release of L-DOPA from cultured rat striatal cells. *J Neurochem* **64:** 487–496.

Geschwind MD, Kessler JA, Geller AI, Federoff HJ (1994). Transfer of the nerve growth factor gene into cell lines and cultured neurons using a defective herpes simplex virus vector. Transfer of the NGF gene into cells by a HSV-1 vector. *Mol Brain Res* **24:** 327–335.

Glorioso JC, Bender MA, Goins WF, Fink DJ, DeLuca N (1995a). HSV as a gene transfer vector for the nervous system. *Molec Biotech* **4:** 87–98.

Glorioso JC, DeLuca NA, Fink DJ (1995b). Development and application of herpes simplex virus vectors for human gene therapy. *Ann Rev Microbiol* **49:** 675–710.

Heeg U, Dienes HP, Muller S, Falke D (1986). Involvement of actin-containing microfilaments in HSV-induced cytopathology and the influence of inhibitors of glycosylation. *Arch Virol* **91:** 257–270.

Ho W, Heinemann C, Hangan D, Uniyal S, Morris VL, Chan BM (1997). Modulation of in vivo migratory function of $\alpha 2\beta 1$ integrin in mouse liver. *Mol Biol Cell* **8:** 1863–1875.

Johnson PA, Friedmann T (1994). Replication-defective recombinant herpes simplex virus vectors. In: Roth MG (ed), *Methods in Cell Biology Volume 43: Protein Expression in Animal Cells*. Academic Press, Toronto, pp 211–230.

Johnson PA, Miyanohara A, Levine F, Cahill T, Freidmann T (1992). Cytotoxicity of a replication-defective mutant of herpes simplex virus type 1. *J Virol* **66:** 2952–2965.

Johnson PA, Wang MJ, Friedman T (1994). Improved cell survival by the reduction of immediate-early gene expression in replication-defective mutants of herpes simplex virus type 1 but not by mutation of the virion host shutoff function. *J Virol* **68:** 6347–6362.

Krassioukov AV, Weaver LC (1995). Episodic hypertension due to autonomic dysreflexia in acute and chronic spinal cord-injured rats. *Am J Physiol* **268:** H2077–H2083.

Krassioukov AV, Weaver LC (1996). Morphological changes in sympathetic preganglionic neurons after spinal cord injury in rats. *Neurosci* **70:** 211–226.

Krempien U, Jockusch BM, Jungwirth C (1984). Herpes simplex virus-induced cell surface protrusions. *Intervirology* **22:** 156–163.

Krenz NR, Weaver LC (1998). Sprouting of primary afferent fibers after spinal cord transection in the rat. *Neurosci* **85:** 443–458.

Krisky DM, Marconi PC, Oligino TJ, Rouse R, Fink DJ, Cohen JB, Watkins SC, Glorioso JC (1998). Development of herpes simplex virus replication-defective multigene vectors for combination gene therapy applications. *Gene Therapy* **5:** 1517–1530.

Krukoff TL, Gehlen F, Ganten D, Wagner J (1995). Gene expression of brain nitric oxide synthase and soluble guanylyl cyclase in hypothalamus and medulla of two-kidney, one clip hypertensive rats. *Hypertension* **26:** 171–176.

Leib DA, Olivo PD (1993). Gene delivery to neurons: Is herpes simplex virus the right tool for the job? *BioEssays* **15:** 547–554.

LeVatte MA, Cassam AK, Dekaban GA, Weaver LC (1998a). Analysis of a multi-mutant herpes simplex virus type 1 for gene transfer into sympathetic preganglionic neurons and a comparison to adenovirus vectors. *Neurosci* **86:** 1321–1336.

LeVatte MA, Dekaban GA, Weaver LC (1997). Gene transfer into sympathetic preganglionic neurons in vivo using a nonreplicating thymidine kinase deficient herpes simplex virus type 1. *Neurosci* **80:** 893–906.

LeVatte MA, Mabon PJ, Weaver LC, Dekaban GA (1998b). Simultaneous identification of two populations of sympathetic preganglionic neurons using recombinant herpes simplex type 1 virus expressing different reporter genes. *Neurosci* **82:** 1253–1267.

LeVatte MA, Weaver LC, York IA, Johnson D, Dekaban GA (1995). Delivery of a foreign gene to sympathetic preganglionic neurons using recombinant herpes simplex virus. *Neurosci* **66:** 737–750.

Llewellyn-Smith IJ, Cassam AK, Krenz NR, Krassioukov AV, Weaver LC (1997). Glutamate- and GABA-immunoreactive synapses on sympathetic preganglionic neurons caudal to a spinal cord transection in rats. *Neurosci* **80:** 1225–1235.

Luque JM, Bleuel Z, Malherbe P, Richards JG (1994). Alternatively spliced isoforms of the N-methyl-D-aspartate receptor subunit 1 are differentially distributed within the rat spinal cord. *Neurosci* **63:** 629–635.

Mabon PJ, LeVatte MA, Dekaban GA, Weaver LC (1997). Identification of sympathetic preganglionic neurons controlling the small intestine in hamsters using a recombinant herpes simplex virus type-1. *Brain Res* **753:** 245–250.

Mabon PJ, Weaver L, Dekaban G (1998). Cyclosporin A reduces the inflammatory response to a multi-mutant herpes simplex virus type-1 leading to improved transgene expression in sympathetic preganglionic neurons in hansters. *J Neurovirol.* **5:** 268–279.

Maiorov DN, Krenz NR, Krassioukov AV, Weaver LC (1997). Role of spinal NMDA and AMPA receptors in episodic hypertension in conscious spinal rats. *Am J Physiol* **273:** H1266–H1274.

Marshall J, Molloy R, Moss GWJ, Howe JR, Hughes TE (1995). The jellyfish green fluorescent protein a new tool for studying ion channel expression and function. *Neuron* **14:** 211–215.

Martin D, Near SL, Bendele A, Russel DA (1995). Inhibition of tumor necrosis factor is protective against neurologic dysfunction after active immunization of Lewis rats with myelin basic protein. *Exp Neurol* **131:** 222–228.

Neve RL, Howe JR, Hong S, Kalb RG (1997). Introduction of the glutamate receptor subunit 1 into motor neurons in vitro and in vivo using recombinant herpes simplex virus. *Neurosci* **79:** 435–447.

Norrild B, Lehto VP, Virtanen I (1986). Organization of cytoskeleton elements during herpes simplex virus type 1 infection of human fibroblasts: An immunofluorescence study. *J Gen Virol* **67:** 97–105.

Oger J, Dekaban GA (1995). HTLV-1 associated myelopathy: a case for viral-induced autoimmunity versus induced inflammation. *Autoimmunity* **21:** 151–159.

Rubenstein R, Price RW (1983). Replication of thymidine kinase deficient herpes simplex virus type 1 neuronal cell cultures: Infection of the PC12 cell. *Arch Virol* **78:** 49–64.

Rubenstein R, Price RW (1984). Early inhibition of acetylcholinesterase and choline acetyltransferase activity in herpes simplex virus type-1 infection of PC12 cells. *J Neurochem* **42:** 142–150.

Rubenstein R, Price RW, Joh T (1985). Alterations of tyrosine hydroxylase activity in PC12 cells infected with herpes simplex virus type 1. *Arch Virol* **83:** 65–82.

Russell J, Stow EC, Stow ND, Preston CM (1987). Abnormal forms of the herpes simplex virus immediate early polypeptide Vmw175 induce the cellular stress response. *J Gen Virol* **68:** 2397–2406.

Sanders MC, Wang YL (1991). Assembly of actin-containing cortex occurs at distal regions of growing neurites in PC12 cells. *J Cell Science* **100:** 771–780.

Sheng M, Wyszynski M (1997). Ion channel targeting in neurons. *BioEssays* **19:** 847–853.

Shering AF, Bain D, Stewart K, Epstein AL, Castro MG, Wilkinson GWG, Lowenstein PR (1997). Cell type-specific expression in brain cell cultures from a short human cytomegalovirus major immediate early promoter depends on whether it is inserted into herpesvirus or adenovirus vectors. *J Gen Virol* **78:** 445–459.

Steiner I, Kennedy PGE (1993). Molecular biology of herpes simplex virus type 1 latency in the nervous system. *Mol Neurobiol* **7:** 137–159.

Sucher NJ, Brose N, Deitcher DL, Awobuluyi M, Gasic GP, Bading H, Cepko CL, Greenberg ME, Jahn R, Heinemann SF, Liption SA (1993). Expression of endogenous NMDAR1 transcripts without receptor protein suggests post-transcriptional control in PC12 cells. *J Biol Chem* **268:** 22299–22304.

Tanabe Y, Roelink H, Jessell T (1995). Induction of motor neurons by Sonic hedgehog is independent of floor plate differentiation. *Current Biology* **5:** 651–658.

Tolle TR, Berthele A, Zieglgansberger W, Seeburg PH, Wisden W (1993). The differential expression of 16 NMDA and non-NMDA receptor subunits in the rat spinal cord and in periaqueductal gray. *J Neurosci* **13:** 5009–5028.

Tomaselli KJ, Hall DE, Flier LA, Gehlsen KR, Turner DC, Carbonetto S, Reichardt LF (1990). A neuronal cell line (PC12) expresses two β1-class integrins $\alpha 1\beta 1$ and $\alpha 3\beta 1$ – that recognize different neurite outgrowth-promoting domains in laminin, *Neuron* **5:** 651–662.

Weaver LC, Cassam AK, Krassioukov AV, Llewellyn-Smith IJ (1997). Changes in immunoreactivity for growth associated protein-43 suggest reorganization of synapses on spinal sympathetic neurons after cord transection. *Neurosci* **81:** 535–551.

Wechsler A, Teichberg VI (1998). Brain spectrin binding to the NMDA receptor is regulated by phosphorylation, calcium and calmodulin. *EMBO J* **17:** 3931–3939.

Wood MJA, Byrnes AP, Pfaff DW, Ratkin SD, Charlton HM (1994). Inflammatory effects of gene transfer into the CNS with defective HSV-1 vectors. *Gene Therapy* **1:** 283–291.

Wyszynski M, Kharazia V, Shanghvi R, Roa A, Beggs AH, Craig AM, Weinberg R, Sheng M (1998). Differential regional expression and ultrastructural localization of -actinin-2, a putative NMDA receptor-anchoring protein, in rat brain. *J Neurosci* **18:** 1383–1392.

Wyszynski M, Lin J, Rao A, Nigh E, Beggs AH, Craig AM, Sheng M (1997). Competitive binding of alpha-actinin and calmodulin to the NMDA receptor. *Nature* **385:** 439–442.